AD-A098 241 SCIENCE APPLICATIONS INC BOULDER CO PLASMA RESEARCH INST F/G 20/5
FREE ELECTRON LASER INSTABILITY FOR A RELATIVISTIC ANNULAR ELEC--ETC(U)
NOV 80 H S UHM, R C DAVIDSON N00014-79-C-0555
UNCLASSIFIED SAI-254-80-626-LJ NL

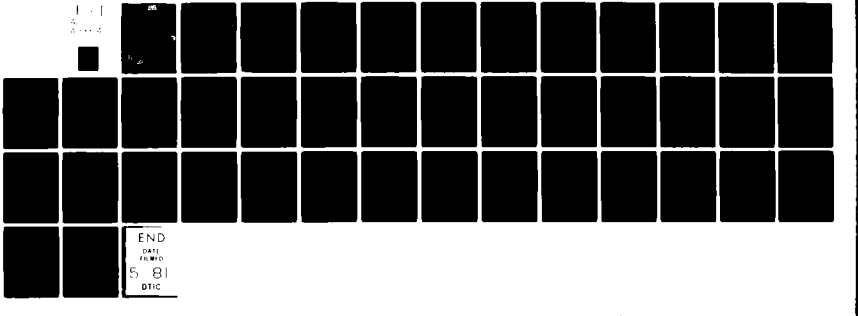

END
DATE FILMED
5 81
DTIC

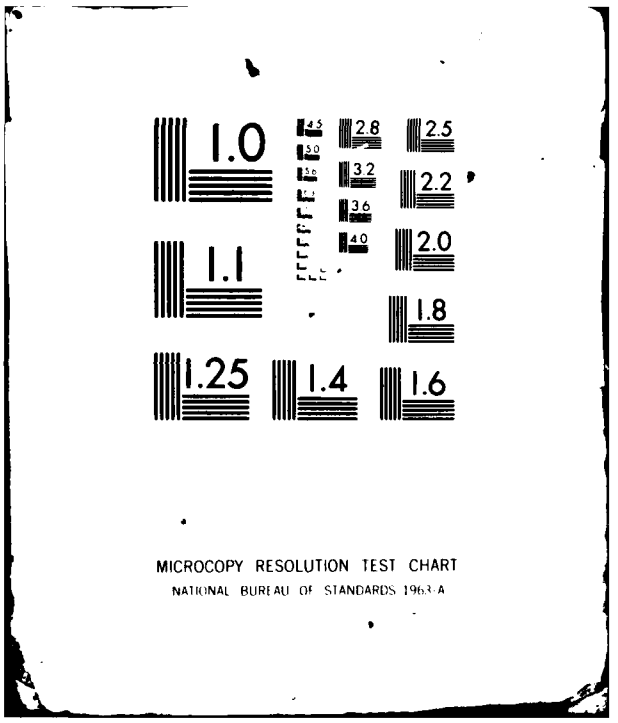
1.0
1.1
1.25
1.4
1.6
1.8
2.0
2.2
2.5
2.8
3.2
3.6
4.0
4.5
5.0
5.6
MICROCOPY RESOLUTION TEST CHART
NATIONAL BUREAU OF STANDARDS 1963-A

SCIENCE APPLICATIONS
Plasma Research Institute, 934 Pearl Street

(12)

SAI-254-80-626-LJ/PRI-17 November 1980

FREE ELECTRON LASER INSTABILITY FOR A RELATIVISTIC ANNULAR ELECTRON BEAM IN A HELICAL WIGGLER FIELD

Han S. Uhm
Naval Surface Weapons Center
White Oak, Silver Spring, Maryland 20910

Ronald C. Davidson
Plasma Fusion Center
Massachusetts Institute of Technology
Cambridge, Massachusetts 02139
and
Science Applications, Inc.
Boulder, Colorado 80302

The free electron laser instability is investigated for a relativistic annular electron beam propagating through a helical wiggler magnetic field. It is assumed that the beam is thin, with radial thickness (2a) much smaller than the beam radius (R_0), and that $\nu/\gamma_b \ll 1$, where ν is Budker's parameter. The stability analysis is carried out within the framework of the linearized Vlasov-Maxwell equations for perturbations with general azimuthal harmonic number ℓ and radial mode number s, including the important influence of (a) finite beam geometry in the radial direction, (b) positioning of the beam radius relative to the outer conducting wall (R_0/R_c), and (c) finite wiggler amplitude (δB). All of these effects are shown to have an important influence on stability behavior. Moreover, the maximum coupling between the transverse and longitudinal modes increases substantially with increasing radial mode number s. It is also found that the transverse magnetic (TM) mode has slightly larger growth rate than the transverse electric (TE) mode.

unclassified

SECURITY CLASSIFICATION OF THIS PAGE (When Data Entered)

REPORT DOCUMENTATION PAGE

READ INSTRUCTIONS BEFORE COMPLETING FORM

1. REPORT NUMBER: SAI-254-80-626-LJ PRI-17	2. GOVT ACCESSION NO. AD-A098241
3. RECIPIENT'S CATALOG NUMBER	
4. TITLE (and Subtitle): FREE ELECTRON LASER INSTABILITY FOR A RELATIVISTIC ANNULAR ELECTRON BEAM IN A HELICAL WIGGLER FIELD,	5. TYPE OF REPORT & PERIOD COVERED: Technical Report
	6. PERFORMING ORG. REPORT NUMBER: PRI-17
7. AUTHOR(s): Han S. Uhm, Ronald C. Davidson	8. CONTRACT OR GRANT NUMBER(s): ONR-N00014-79-C-0555
9. PERFORMING ORGANIZATION NAME AND ADDRESS: Science Applications, Inc., Plasma Research Institute, 934 Pearl Street, Boulder, Colorado 80302	10. PROGRAM ELEMENT, PROJECT, TASK AREA & WORK UNIT NUMBERS
11. CONTROLLING OFFICE NAME AND ADDRESS: Office of Naval Research, Physics Program Office, Arlington, VA 22217	12. REPORT DATE: November 1980 13. NUMBER OF PAGES: 39
14. MONITORING AGENCY NAME & ADDRESS (if different from Controlling Office)	15. SECURITY CLASS. (of this report): unclassified 15a. DECLASSIFICATION/DOWNGRADING SCHEDULE

16. DISTRIBUTION STATEMENT (of this Report)

Approved for public release: distribution unlimited

17. DISTRIBUTION STATEMENT (of the abstract entered in Block 20, if different from Report)

18. SUPPLEMENTARY NOTES

19. KEY WORDS (Continue on reverse side if necessary and identify by block number)

relativistic electron beam for free electron laser

20. ABSTRACT (Continue on reverse side if necessary and identify by block number)

The free electron laser instability is investigated for a relativistic annular electron beam propagating through a helical wiggler magnetic field. It is assumed that the beam is thin, with radial thickness (2a) much smaller than the beam radius (R_o), and that $\nu/\gamma_b \ll 1$, where ν is Budker's parameter. The stability analysis is carried out within the framework of the linearized Vlasov-Maxwell equations for perturbations with general azimuthal harmonic number ℓ and radial mode number s, including the important influence of (a) finite beam

DD FORM 1 JAN 73 1473 EDITION OF 1 NOV 65 IS OBSOLETE

S/N 0102-LF-014-6601

unclassified

SECURITY CLASSIFICATION OF THIS PAGE (When Data Entered)

411950

20. Abstract, continued.

geometry in the radial direction, (b) positioning of the beam radius relative to the outer conducting wall (R_o/R_c) and (c) finite wiggler amplitude (δB). All of these effects are shown to have an important influence on stability behavior. Moreover, the maximum coupling between the transverse and longitudinal modes increases substantially with increasing radial mode number s. It is also found that the transverse magnetic (TM) mode has slightly larger growth rate than the transverse electric (TE) mode.

I. INTRODUCTION

There is a growing literature on the free electron laser[1-7] which generates coherent electromagnetic radiation using a relativistic electron beam. For the most part, previous theoretical analyses of this instability have been carried out for an electron beam with uniform density, neglecting the influence of finite radial geometry.[3-6] Strictly speaking, a more accurate theoretical model of radiation generation by the free electron laser instability, including a determination of the optimum value of the beam radius R_0, requires a linear stability analysis for perturbations about an annular electron beam propagating in a helical wiggler magnetic field. This paper develops a self-consistent theory of the free electron laser instability for a relativistic annular electron beam propagating in a helical wiggler field, allowing for perturbations with general azimuthal harmonic number ℓ. The present work extends the previous analysis[7] by the authors, carried out for an undulator (multiple mirror) wiggler field and $\ell = 0$ perturbations, to the case of a helical wiggler field and arbitrary azimuthal harmonic number ℓ.

The analysis is carried out within the framework of the Vlasov-Maxwell equations for a relativistic annular electron beam propagating in the combined transverse wiggler and uniform axial guide fields described by

$$\underset{\sim}{B}^0 = B_0\hat{\underset{\sim}{e}}_z - \delta B\cos k_0 z\,\hat{\underset{\sim}{e}}_x - \delta B\sin k_0 z\,\hat{\underset{\sim}{e}}_y ,$$

where B_0 and δB are constants, $\lambda_0 = 2\pi/k_0$ is the axial wavelength of the helical wiggler field, and $\hat{\underset{\sim}{e}}_x$, $\hat{\underset{\sim}{e}}_y$, and $\hat{\underset{\sim}{e}}_z$ are unit vectors in the x-, y-, and z-directions, respectively. It is assumed that the beam thickness (2a) is much smaller than the mean beam radius R_0,

and that $\nu/\gamma_b \ll 1$, where ν is Budker's parameter, and $\gamma_b mc^2$ is the characteristic energy of the electron beam. In Sec. II, equilibrium properties are calculated for the choice of equilibrium distribution function [Eq. (14)]

$$f_b^0 = K \times \delta(C_h - C_0)\delta(C_\perp - \gamma_b^2 m^2 v_0^2)G(C_z) ,$$

where C_h, $C_\perp$, and C_z are the helical, transverse, and axial invariants[8] defined in Eqs. (12), (11), and (13), respectively, K is a normalization constant, and v_0 and C_0 are constants related to the radial thickness and mean radius, respectively, of the beam.

The formal stability analysis for the free electron laser instability is carried out in Sec. III, and a complete dispersion relation [Eq. (68)] is obtained, assuming that $|\omega - (k + nk_0)\beta_b c| \ll k_0\beta_b c, \omega_c$, where ω and $k + nk_0$ are the complex oscillation frequency and the wavenumber of the perturbation, respectively, $\omega_c = eB_0/\gamma_b mc$ is the electron cyclotron frequency, c is the speed of light in vacuo, and $\beta_b c = (\gamma_b^2 - 1)^{1/2} c/\gamma_b$ is the mean axial velocity of the electron beam. The resulting dispersion relation [Eq. (68)] constitutes one of the principal results of this paper and can be used to investigate stability properties for a broad range of system parameters.

In Sec. IV, the dispersion relation for the free electron laser instability is investigated for ω and $k + nk_0$ near the simultaneous zeroes of the transverse (vacuum waveguide) dispersion relation,

$$\left(\frac{\omega^2}{c^2} - (k + nk_0 - k_0)^2\right) R_c^2 = \begin{cases} \alpha_{\ell+1,s}^2 , & \text{TE mode,} \\ \beta_{\ell+1,s}^2 , & \text{TM mode,} \end{cases}$$

and the longitudinal dispersion relation $\Gamma_{\ell,n} + (\pi/2\gamma_b^2)\chi_{n,n} = 0$, where R_c is the radius of the conducting wall, $\Gamma_{\ell,n}$ and $\chi_{n,n'}$ are defined in Eqs. (54) and (81) and $\beta_{\ell',s}$ and $\alpha_{\ell',s}$ are the s'th roots

of the Bessel function $J_{\ell'}(\beta_{\ell',s}) = 0$ and its derivative $J'_{\ell'}(\alpha_{\ell',s}) = 0$, respectively. The abbreviations TE and TM refer to transverse electric and transverse magnetic polarizations, respectively. It is shown that the maximum coupling between the longitudinal and transverse modes occurs at a value of R_0 satisfying

$$R_0/R_c = \begin{cases} \alpha_{\ell,1}/\alpha_{\ell+1,s} , & \text{TE mode,} \\ \alpha_{\ell,1}/\beta_{\ell+1,s} , & \text{TM mode .} \end{cases}$$

Moreover, the coupling coefficient increases considerably with increasing radial mode number s. It is also found that the TM mode is slightly more unstable than the TE mode.

II. EQUILIBRIUM CONFIGURATION AND ASSUMPTIONS

The equilibrium configuration consists of a relativistic annular electron beam propagating in the combined transverse wiggler and uniform axial guide fields described by

$$\underset{\sim}{B}^0 = B_0\hat{\underset{\sim}{e}}_z + \delta\underset{\sim}{B}$$

$$= B_0\hat{\underset{\sim}{e}}_z - \delta B\cos k_0 z\hat{\underset{\sim}{e}}_x - \delta B\sin k_0 z\hat{\underset{\sim}{e}}_y \ , \qquad (1)$$

where B_0 and δB are constants, $\lambda_0 = 2\pi/k_0$ = const. is the axial wavelength of the helical wiggler field, and $\hat{\underset{\sim}{e}}_x$, $\hat{\underset{\sim}{e}}_y$, and $\hat{\underset{\sim}{e}}_z$ are unit vectors in the x-, y-, and z-directions, respectively. The electron beam has a characteristic radial thickness 2a and mean radius R_0, and is located inside a grounded cylindrical conducting wall with radius R_c. We introduce cylindrical polar coordinates (r,θ,z) with z-axis along the axis of the beam; r is the radial distance from the z-axis, and θ is the polar angle in a plane perpendicular to the z-axis. In cylindrical coordinates, the transverse wiggler field $\delta\underset{\sim}{B}$ in Eq. (1) can be expressed as

$$\delta\underset{\sim}{B} = \delta B_r\hat{\underset{\sim}{e}}_r + \delta B_\theta\hat{\underset{\sim}{e}}_\theta$$

$$= -\delta B\cos(\theta - k_0 z)\hat{\underset{\sim}{e}}_r + \delta B\sin(\theta - k_0 z)\hat{\underset{\sim}{e}}_\theta \ , \qquad (2)$$

where $\hat{\underset{\sim}{e}}_r$ and $\hat{\underset{\sim}{e}}_\theta$ are unit vectors in the r- and θ- directions, respectively. To make the analysis tractable, the following simplifying assumptions are made.

(a) The thickness of the annular electron beam is much smaller than its mean radius, i.e.,

$$a/R_0 \ll 1. \qquad (3)$$

(b) The characteristic transverse momentum $\underset{\sim}{p}_\perp$ of a beam electron is small in comparison with the characteristic directed axial momentum $\gamma_b m V_b$, i.e.,

$$|\underset{\sim}{p}_\perp| \ll \gamma_b m V_b \simeq p_z \ , \tag{4}$$

where V_b is the mean axial velocity of the electron beam.

(c) It is also assumed that

$$\nu/\gamma_b \ll 1, \tag{5}$$

where $\gamma_b mc^2$ is the characteristic electron energy, and $\nu = N_b e^2/mc^2$ is Budker's parameter. Here, c is the speed of light in vacuo, -e and m are the electron charge and rest mass, respectively, and $N_b = \int_0^{2\pi} d\theta \int_0^\infty dr\ r\ n_b^0$ is the number of electrons per unit axial length. Consistent with Eq. (5), the equilibrium self fields can be neglected in comparison with the applied magnetic field $\underset{\sim}{B}^0$ in Eq. (1).

(d) It is assumed that the axial wavelength $\lambda_0 = 2\pi/k_0$ of the helical wiggler field is sufficiently short that

$$\frac{\omega_c^2}{|\omega_0 - \omega_c|^2} \frac{\delta B^2}{B_0^2} \lesssim k_0^2 a^2 \ , \tag{6}$$

where ω_0 and ω_c are defined by

$$\omega_0 = k_0 V_b \text{ and } \omega_c = \frac{eB_0}{\gamma_b mc} \ . \tag{7}$$

Consistent with Eq. (6), it is also assumed that

$$\frac{2\omega_c\omega_0}{|\omega_0 - \omega_c|^2} \left| \frac{\underset{\sim}{p}_\perp}{\gamma_b m V_b} \cdot \frac{\delta \underset{\sim}{B}}{B_0} \right| \ll 1 \ , \tag{8}$$

which is easy to satisfy for sufficiently short wiggler wavelengths.

(e) In the stability analysis, it is assumed that the wave perturbations are far removed from resonance with the transverse

cyclotron motion and the axial motion of the beam, i.e.,

$$|\omega - (k + nk_0)V_b| \ll \omega_c, k_0 V_b, \tag{9}$$

where ω is the complex oscillation frequency, and $k + nk_0$ is the wavenumber of the perturbation. It is also assumed that the cyclotron motion and the axial motion is nonresonant with

$$k_0^2 v_z^2 \neq \omega_c^2 , \tag{10}$$

where $v_z = p_z/\gamma m$ is the axial velocity of a typical beam electron.

Within the context of Assumption (c), there are three exact invariants[8] associated with the single-particle motion in the equilibrium field $\underset{\sim}{B}^0$ [Eq. (1)]. These are the transverse invariant $C_\perp$,

$$C_\perp = p_r^2 + p_\theta^2 + \frac{2eB_0}{ck_0}(p_z - \gamma_b m V_b) + \frac{2e}{ck_0}\underset{\sim}{p}_\perp \cdot \delta\underset{\sim}{B}, \tag{11}$$

the helical invariant C_h,

$$C_h = P_\theta + \frac{1}{k_0}(p_z - \gamma_b m V_b) + \frac{e\delta B}{ck_0} r\sin(\theta - k_0 z) , \tag{12}$$

and the axial invariant C_z defined by

$$\left(C_z - \frac{eB_0}{ck_0}\right)^2 = \left(p_z - \frac{eB_0}{ck_0}\right)^2 - \frac{2e}{ck_0}\underset{\sim}{p}_\perp \cdot \delta\underset{\sim}{B} , \tag{13}$$

where $\underset{\sim}{p} = (p_r, p_\theta, p_z) = \gamma m \underset{\sim}{v}$ is the mechanical momentum, $P_\theta = r(p_\theta - eB_0 r/2c)$ is the canonical angular momentum associated with the axial field B_0, $\gamma mc^2 = (m^2c^4 + c^2\underset{\sim}{p}^2)^{1/2}$ is the relativistic electron energy, and $\gamma_b = (1 - v_b^2/c^2)^{-1/2} = \text{const}$.

In the present analysis, we consider the general class of annular electron beam equilibria described by[8]

$$f_b^0 = K\,\delta(C_\perp - \gamma_b^2 m^2 v_0^2)\delta(C_h - C_0)G(C_z) , \tag{14}$$

where v_0 is a constant related to the radial thickness of the beam,

K is a positive normalization constant, C_0 = const. is defined by

$$C_0 = -\frac{1}{2}\frac{eB_0}{c}R_0^2 , \tag{15}$$

and $G(C_z)$ is normalized according to

$$\int_{-\infty}^{\infty} dC_z G(C_z) = 1. \tag{16}$$

In the parameter regimes of practical interest for free electron laser applications, $G(C_z)$ is strongly peaked around $C_z = \gamma_b mV_b$, with characteristic half-width $\Delta C_z \ll \gamma_b mV_b$. We therefore approximate Eq. (13) by[8]

$$C_z = p_z - \frac{\omega_c}{\omega_0 - \omega_c} \underset{\sim}{p}_\perp \cdot \frac{\delta \underset{\sim}{B}}{B_0} , \tag{17}$$

where use has been made of Eq. (8).

As a simple example, we consider the distribution function in which all electrons have a same value of axial invariant C_z, i.e.,

$$G(C_z) = \delta(C_z - \gamma_b mV_b) . \tag{18}$$

After some straightforward algebraic manipulation that makes use of Eqs. (3), (6), (15), and (17), it can be shown that the electron density profile associated with the distribution function in Eqs. (14) and (18) can be approximated by[8]

$$n_b^0(r) = \begin{cases} \dfrac{N_b/\pi^2}{[(r^2 - r_1^2)(r_2^2 - r^2)]^{1/2}} , & r_1 \le r \le r_2 , \\ 0 , & \text{otherwise} , \end{cases} \tag{19}$$

where $r_1 = R_0 - r_L$, $r_2 = R_0 + r_L$, and the effective Larmor radius r_L is defined by

$$r_L^2 = \frac{v_0^2}{\omega_c^2} + \frac{v_b^2}{(\omega_0 - \omega_c)^2}\left(\frac{\delta B}{B_0}\right)^2 . \qquad (20)$$

In the lowest order calculation presented here, the electron density profile in Eq. (19) is independent of θ and z for system parameters satisfying Eqs. (3) and (6). Additional equilibrium properties associated with the distribution function in Eq. (14) are discussed in Ref. 8.

III. LINEARIZED VLASOV-MAXWELL EQUATIONS

In this section, we make use of the linearized Vlasov-Maxwell equations to obtain an eigenvalue equation describing the free electron laser instability in an annular electron beam. In the subsequent analysis, it is assumed that all perturbed quantities have temporal and spatial variations of the form

$$\delta\psi(\underset{\sim}{x},t) = \delta\hat{\psi}(\underset{\sim}{x})\exp(-i\omega t) ,$$

where $\mathrm{Im}\omega > 0$, and $\psi(\underset{\sim}{x})$ is the amplitude of the perturbation. Using the method of characteristics, and neglecting initial perturbations, the perturbed electron distribution function is given by

$$\delta f_b(\underset{\sim}{x},\underset{\sim}{p},t) = e\int_{-\infty}^{t} dt' \left(-\nabla'\delta\phi(\underset{\sim}{x}',t') - \frac{1}{c}\frac{\partial}{\partial t'}\delta\underset{\sim}{A}(\underset{\sim}{x}',t') + \frac{\underset{\sim}{v}' \times \nabla' \times \delta\underset{\sim}{A}(\underset{\sim}{x}',t')}{c}\right) \cdot \frac{\partial}{\partial \underset{\sim}{p}'} f_b^0(\underset{\sim}{x}',\underset{\sim}{p}') , \tag{21}$$

where $d\underset{\sim}{x}'/dt' = \underset{\sim}{v}'$ and $d\underset{\sim}{p}'/dt' = -e\underset{\sim}{v}' \times \underset{\sim}{B}^0(\underset{\sim}{x}')/c$, and the particle trajectories $(\underset{\sim}{x}', \underset{\sim}{p}')$ in the equilibrium field configuration satisfy the "initial" condition $\underset{\sim}{x}'(t' = t) = \underset{\sim}{x}$ and $\underset{\sim}{p}'(t' = t) = \underset{\sim}{p}$. In Eq. (21), the perturbed electric and magnetic potentials, $\delta\phi$ and $\delta\underset{\sim}{A}$, are determined self-consistently from the linearized Maxwell equations

$$\left(\nabla^2 - \frac{1}{c^2}\frac{\partial^2}{\partial t^2}\right)\delta\phi = 4\pi e\int d^3p\ \delta f_b , \tag{22}$$

and

$$\left(\nabla^2 - \frac{1}{c^2}\frac{\partial^2}{\partial t^2}\right)\delta\underset{\sim}{A} = \frac{4\pi e}{c}\int d^3p\ \underset{\sim}{v}\ \delta f_b , \tag{23}$$

respectively, where use has been made of the Lorentz gauge condition

$$\nabla \cdot \delta\underset{\sim}{A}(\underset{\sim}{x},t) + \frac{1}{c}\frac{\partial}{\partial t}\delta\phi(\underset{\sim}{x},t) = 0 . \tag{24}$$

Without loss of generality, the perturbation amplitudes are expanded according to

$$\delta\hat{\psi}(\underset{\sim}{x}) = \sum_{\ell=-\infty}^{\infty} \sum_{n=-\infty}^{\infty} \psi_{\ell}^{(n)}(r)\exp\{i[\ell\theta + (k + nk_0)z]\} \ . \tag{25}$$

Correct to lowest order, the axial motion of the electrons is free-streaming, i.e.,

$$z' = z + \frac{p_z}{\gamma m}(t' - t) \ . \tag{26}$$

The transverse trajectories are calculated for the case where the wiggler amplitude satisfies Eq. (6), assuming that the axial and transverse motions are far removed from cyclotron resonance, i.e., $k_0^2 v_z^2 \neq \omega_c^2$ [Eq. (10)]. After some straightforward algebra,[7,8] we obtain

$$v_r' = v_r\cos\omega_c\tau - (r - R_0)\omega_c\sin\omega_c\tau$$

$$+ \frac{\omega_c}{\omega_c - \omega_0}\frac{\delta B}{B_0}\{- v_z\cos(\theta - k_0 z - k_0 v_z\tau)$$

$$+ [(\omega_c/k_0)\sin(\theta - k_0 z)\sin\omega_c\tau + v_z\cos(\theta - k_0 z)\cos\omega_c\tau]\} \ , \tag{27}$$

and

$$v_\theta' = (r - R_0)\omega_c\cos\omega_c\tau + v_r\sin\omega_c\tau$$

$$+ \frac{\omega_c}{\omega_c - \omega_0}\frac{\delta B}{B_0}\{v_z\sin(\theta - k_0 z - k_0 v_z\tau)$$

$$- [(\omega_c/k_0)\sin(\theta - k_0 z)\cos\omega_c\tau - v_z\cos(\theta - k_0 z)\sin\omega_c\tau]\} \ , \tag{28}$$

where use has been made of Eqs. (12) and (26), and $\tau = t' - t$.

As evident from Eqs. (27) and (28), the radial and azimuthal orbits contain oscillatory contributions proportional to $\cos\omega_c\tau$, $\sin\omega_c\tau$, $\sin(\theta - k_0 z - k_0 v_z\tau)$ and $\cos(\theta - k_0 z - k_0 v_z\tau)$. For present

purposes, in the t'-integration on the right-hand side of Eq. (21), we retain terms proportional to $[\omega - (k + nk_0)p_z/\gamma m]^{-1}$, and assume that the value of $[\omega - (k + nk_0)p_z/\gamma m]$ is well removed from resonance with the cyclotron motion and the axial motion of the beam [Eq. (9)], i.e.,

$$|\omega - (k + nk_0)p_z/\gamma m| \ll \omega_c , \quad k_0 V_b .$$

Within the context of Eqs. (1) and (9), the perturbed distribution function in Eq. (21) can be approximated by[7]

$$\delta\hat{f}_b(\underset{\sim}{x},\underset{\sim}{p}) = -e\int_{-\infty}^{0} d\tau \exp(-i\omega\tau) \left\{ 2\left[\gamma m i\omega(\delta\hat{\phi} - \frac{1}{c}\,\underset{\sim}{v}' \cdot \delta\hat{\underset{\sim}{A}}) \right.\right. \\ \left.\left. -p_z\left(\frac{\partial}{\partial z}\,\delta\hat{\phi} - \frac{1}{c}\,\underset{\sim}{v}' \cdot \frac{\partial}{\partial z}\,\delta\hat{\underset{\sim}{A}} \right) \right] \frac{\partial f_b^0}{\partial p_\perp^2} + \left(\frac{\partial}{\partial z}\,\delta\hat{\phi} - \frac{1}{c}\,\underset{\sim}{v}' \cdot \frac{\partial}{\partial z}\,\delta\hat{\underset{\sim}{A}} \right) \cdot \frac{\partial f_b^0}{\partial p_z} \right\} , \tag{29}$$

where $\gamma = H/mc^2 = (1 + \underset{\sim}{p}^2/m^2c^2)^{1/2}$. Moreover, making use of Eq. (9), only those contributions to v_r' and v_θ' proportional to $\sin(\theta - k_0 z - k_0 v_z \tau)$ and $\cos(\theta - k_0 z - k_0 v_z \tau)$ are retained. That is, on the right-hand side of Eq. (29), we retain contributions to v_r' and v_θ' of the form

$$v_r' = v_z \frac{\omega_c}{\omega_0 - \omega_c} \frac{\delta B}{B_0} \cos(\theta - k_0 z - k_0 v_z \tau) , \tag{30}$$

and

$$v_\theta' = -v_z \frac{\omega_c}{\omega_0 - \omega_c} \frac{\delta B}{B_0} \sin(\theta - k_0 z - k_0 v_z \tau) . \tag{31}$$

Finally, since the oscillatory modulation of the radial and azimuthal orbits is small-amplitude [Eqs. (3), (6), and (9)], we approximate

$$r' = r , \quad \theta' = \theta , \tag{32}$$

in the arguments of the perturbation amplitudes on the right-hand side of Eq. (29), i.e.,

$$\psi_\ell^{(n)}(r')\exp(i\ell\theta') \simeq \psi_\ell^{(n)}(r)\exp(i\ell\theta) .$$

Substituting Eqs. (25) and (30) - (32) into Eq. (29), and making use of Eq. (9), we find after some straightforward algebra that the perturbed distribution function $\delta\hat{f}_b(\underset{\sim}{x},\underset{\sim}{p})$ can be approximated by

$$\delta\hat{f}_b(\underset{\sim}{x},\underset{\sim}{p}) = e \sum_{\ell,n} \frac{\exp\{i[\ell\theta + (k + nk_0)z]\}}{\omega - (k + nk_0)v_z} \left\{\lambda_n\left(\phi_\ell^{(n)} - \frac{v_z}{c} A_{z,\ell}^{(r)}\right)\right.$$

$$+ \frac{i}{2}\frac{v_z}{c}\frac{\omega_c}{\omega_c - \omega_0}\frac{\delta B}{B_0}\left[\lambda_{n+1}A_{\theta,\ell-1}^{(n+1)} - \lambda_{n-1}A_{\theta,\ell+1}^{(n-1)}\right]$$

$$\left. + \frac{1}{2}\frac{v_z}{c}\frac{\omega_c}{\omega_c - \omega_0}\frac{\delta B}{B_0}\left[\lambda_{n+1}A_{n,\ell-1}^{(n+1)} + \lambda_{n-1}A_{n,\ell+1}^{(n-1)}\right]\right\}, \tag{33}$$

where the function $\lambda_{n'}(\underset{\sim}{p},\omega,k)$ is defined by

$$\lambda_{n'}(\underset{\sim}{p},\omega,k) = 2[\gamma m\omega - (k + n'k_0)p_z]\frac{\partial f_b^0}{\partial p_\perp^2} + (k + nk_0)\frac{\partial f_b^0}{\partial p_z}. \tag{34}$$

It is convenient to introduce the dimensionless potential amplitudes defined by

$$\hat{\phi}_\ell(r) = \frac{e}{mc^2}\left[\phi_\ell^{(n)}(r) - \frac{v_b}{c}A_{z,\ell}^{(n)}(r)\right], \tag{35}$$

$$\hat{A}_{\theta,\ell\pm1}(r) = \frac{e}{mc^2}A_{\theta,\ell\pm1}^{(n\mp1)}(r), \tag{36}$$

and

$$\hat{A}_{r,\ell\pm1}(r) = \frac{e}{mc^2}A_{r,\ell\pm1}^{(n\mp1)}(r). \tag{37}$$

Moreover, we introduce the dimensionless parameter

$$\Lambda = \frac{e\delta B}{2\gamma_b mc^2 k_0}, \tag{38}$$

and define the effective susceptibility $\chi_{n,n'}(\omega,k)$ by

$$\chi_{n,n'}(\omega,k) = 4\pi e^2\int_0^{R_c} rdr\int d^3p\,\frac{\lambda_{n'}(\underset{\sim}{p},\omega,k)}{\omega - (k + nk_0)v_z}. \tag{39}$$

To simplify the present analysis, it is also assumed that

$$\omega_0 >> \omega_c \ , \tag{40}$$

where $\omega_0 \equiv k_0 V_b$ and $\omega_c = eB_0/\gamma_b mc$. Equation (40) is easily satisfied in parameter regimes of practical interest for free electron laser applications.

The integral $\int d^3p v_z \delta\hat{f}_b$ in Eq. (23) is required to evaluate the r-, θ-, and z-components of the perturbed current density. Within the context of Eqs. (3), (6), and (9), it is important to note from Eqs. (11) and (14) that the quantity $\lambda_n(\underline{p},\omega,k)$ defined in Eq. (34) is an even function of $p_r - p_{r0}$, where[8]

$$p_{r0} = 2\gamma_b mc \frac{\omega_0}{\omega_0 - \omega_c} A\cos(\theta - k_0 z) \ . \tag{41}$$

Therefore, it follows from Eq. (33) that

$$\int d^3p \ v_r \ \delta\hat{f}_b = \int d^3p (p_{r0}/\gamma_b m) \delta\hat{f}_b \ ,$$

where we have approximated $\gamma \simeq \gamma_b$, which is consistent with Eq. (9). That is, the perturbed radial current is given approximately by

$$-e\int d^3p \ v_r \ \delta\hat{f}_b = -2ecA\cos(\theta - k_0 z)\delta\hat{n}_b \ , \tag{42}$$

where use has been made of Eq. (40). It can also be shown that the perturbed azimuthal current is given approximately by

$$-e\int d^3p v_\theta \delta\hat{f}_b = 2ecA\sin(\theta - k_0 z)\delta\hat{n}_b \ . \tag{43}$$

Making use of Eqs. (33) - (43), the Maxwell equations (22) and (23) can be expressed in the approximate form

$$\left\{\frac{1}{r}\frac{\partial}{\partial r}\,r\,\frac{\partial}{\partial r} - \frac{\ell^2}{r^2} + \frac{\omega^2}{c^2} - (k + nk_0)^2\right\}\hat{\phi}_\ell(r) = \frac{\delta(r - R_0)}{\gamma_b^2 R_0}\,\sigma(\omega,k)\ , \tag{44}$$

$$\left\{\frac{1}{r}\frac{\partial}{\partial r}\,r\,\frac{\partial}{\partial r} - \frac{(\ell+1)^2 + 1}{r^2} + \frac{\omega^2}{c^2} - [k + (n-1)k_0]^2\right\}\hat{A}_{r,\ell+1}(r)$$

$$- \frac{2i(\ell+1)}{r^2}\,\hat{A}_{\theta,\ell+1}(r) = \frac{\delta(r - R_0)}{R_0}\,\Lambda\sigma(\omega,k)\ , \tag{45}$$

$$\left\{\frac{1}{r}\frac{\partial}{\partial r}\,r\,\frac{\partial}{\partial r} - \frac{(\ell+1)^2 + 1}{r^2} + \frac{\omega^2}{c^2} - [k + (n-1)k_0]^2\right\}\hat{A}_{\theta,\ell+1}(r)$$

$$+ \frac{2i(\ell+1)}{r^2}\,\hat{A}_{r,\ell+1}(r) = \frac{\delta(r-R_0)}{R_0}(i\Lambda)\sigma(\omega,k)\ , \tag{46}$$

$$\left\{\frac{1}{r}\frac{\partial}{\partial r}\,r\,\frac{\partial}{\partial r} - \frac{(\ell-1)^2 + 1}{r^2} + \frac{\omega^2}{c^2} - [k + (n+1)k_0]^2\right\}\hat{A}_{r,\ell-1}(r)$$

$$- \frac{2i(\ell-1)}{r^2}\,\hat{A}_{\theta,\ell-1}(r) = \frac{\delta(r - R_0)}{R_0}\,\Lambda\sigma(\omega,k)\ , \tag{47}$$

$$\left\{\frac{1}{r}\frac{\partial}{\partial r}\,r\,\frac{\partial}{\partial r} - \frac{(\ell-1)^2 + 1}{r^2} + \frac{\omega^2}{c^2} - [k + (n+1)k_0]^2\right\}\hat{A}_{\theta,\ell-1}(r)$$

$$+ \frac{2i(\ell-1)}{r^2}\,\hat{A}_{r,\ell-1}(r) = \frac{\delta(r - R_0)}{R_0}\,(-i\Lambda)\sigma(\omega,k)\ , \tag{48}$$

for a thin annular beam satisfying Eq. (3). In Eqs. (44) - (48), the source function $\sigma(\omega,k)$ is defined by

$$\sigma(\omega,k) = \chi_{n,n}\hat{\phi}_\ell(R_0) - i\Lambda\left[\chi_{n,n+1}\hat{A}_{\theta,\ell-1}(R_0) - \chi_{n,n-1}\hat{A}_{\theta,\ell+1}(R_0)\right]$$

$$- \Lambda\left[\chi_{n,n+1}\hat{A}_{r,\ell-1}(R_0) + \chi_{n,n-1}\hat{A}_{r,\ell+1}(R_0)\right]\ . \tag{49}$$

Since the right-hand side of Eq. (44) vanishes except at $r = R_0$, Eq. (44) can be expressed as

$$\left(\frac{1}{r}\frac{\partial}{\partial r}\,r\,\frac{\partial}{\partial r} - \frac{\ell^2}{r^2} + p_n^2\right)\hat{\phi}_\ell(r) = 0\ , \tag{50}$$

for $r \neq R_0$. In Eq. (57), the parameter p_n^2 is defined by

$$p_n^2 = \omega^2/c^2 - (k + nk_0)^2 \ . \tag{51}$$

The solution to Eq. (50) is given by

$$\hat{\phi}_n(r) = \begin{cases} AJ_\ell(p_n r) + BN_\ell(p_n r) \ , & R_0 < r \leq R_c \ , \\ CJ_\ell(p_n r) \ , & 0 \leq r < R_0 \ , \end{cases} \tag{52}$$

where $J_\ell(x)$ and $N_\ell(x)$ are Bessel functions of the first and second kind, respectively, of order ℓ, R_c is the radius of the conducting wall, and the constants A, B, and C are determined from the appropriate boundary conditions. Multiplying Eq. (44) by r and integrating from $R_0(1-\epsilon)$ to $R_0(1+\epsilon)$, with $\epsilon \to 0_+$, we obtain[7]

$$\Gamma_{\ell,n}(\omega,k)\hat{\phi}_\ell(R_0) = -\frac{\pi}{2\gamma_b^2}\sigma(\omega,k) \ , \tag{53}$$

where the longitudinal dielectric function $\Gamma_{\ell,n}(\omega,k)$ is defined by

$$\Gamma_{\ell,n}(\omega,k) = \frac{J_\ell(\zeta_n)/J_\ell(\xi_n)}{J_\ell(\xi_n)N_\ell(\zeta_n) - J_\ell(\zeta_n)N_\ell(\xi_n)} \ , \tag{54}$$

with $\xi_n = p_n R_0$ and $\zeta_n = R_c p_n$.

The transverse dielectric functions associated with Eqs. (45) - (48) are calculated in detail in Appendix A. For example, for $0 \leq r < R_0$, the solutions to Eqs. (45) and (46) are given by

$$\begin{aligned} \hat{A}_{r,\ell+1}(r) &= C_-^{(\ell+1)}J_\ell(p_{n-1}r) + C_+^{(\ell+1)}J_{\ell+2}(p_{n-1}r) \ , \\ \hat{A}_{\theta,\ell+1}(r) &= iC_-^{(\ell+1)}J_\ell(p_{n-1}r) - iC_+^{(\ell+1)}J_{\ell+2}(p_{n-1}r) \ , \end{aligned} \tag{55}$$

where $p_{n-1}^2 = \omega^2/c^2 - [k + (n-1)/k_0]^2$, and the constants $C_\pm^{(\ell+1)}$ are determined from the appropriate boundary conditions. After some straightforward algebraic manipulation, which is summarized in

Appendix A, it can be shown from Eqs. (45) and (46) that

$$D^{+}_{\ell+1}(\omega,k)C^{(\ell+1)}_{+}J_{\ell+2}(\xi_{n-1}) = \frac{1}{2}\Lambda\sigma(\omega,k) \ , \tag{56}$$

and

$$D^{-}_{\ell+1}(\omega,k)C^{(\ell+1)}_{-}J_{\ell}(\xi_{n-1}) = \frac{1}{2}\Lambda\sigma(\omega,k) \ , \tag{57}$$

where the transverse dielectric functions $D^{+}_{\ell+1}(\omega,k)$ and $D^{-}_{\ell+1}(\omega,k)$ are defined by

$$D^{+}_{\ell+1}(\omega,k) = -\frac{\zeta_{n-1}J_{\ell+1}(\zeta_{n-1})J'_{\ell+1}(\zeta_{n-1})}{J_{\ell}(\xi_{n-1})J_{\ell+2}(\xi_{n-1})} \ , \tag{58}$$

and

$$D^{-}_{\ell+1}(\omega,k) = \frac{g_{\ell+1}(\zeta_{n-1})/\pi J_{\ell}(\xi_{n-1})}{g_{\ell+1}(\zeta_{n-1})N_{\ell}(\xi_{n-1}) - J_{\ell}(\xi_{n-1})} \ . \tag{59}$$

Here, the prime (') denotes $(d/dx)J_{\ell+1}(x)$. In Eqs. (58) and (59), $\zeta^2_{n'} = [\omega^2/c^2 - (k + n'k_0)^2]R_c^2$, $\xi^2_{n'} = [\omega^2/c^2 - (k + n'k_0)^2]R_0^2$, and the function $g_{\ell'}(\zeta)$ is defined by

$$g_{\ell'}(\zeta) = \frac{2J_{\ell'}(\zeta)J'_{\ell'}(\zeta)}{J_{\ell'}(\zeta)N'_{\ell'}(\zeta) + J'_{\ell'}(\zeta)N_{\ell'}(\zeta)} \ . \tag{60}$$

Similarly, the solutions to the coupled differential equations (47) and (48) are given by

$$\begin{aligned} \hat{A}_{r,\ell-1}(r) &= C^{(\ell-1)}_{-}J_{\ell-2}(p_{n+1}r) + C^{(\ell-1)}_{+}J_{\ell}(p_{n+1}r) \ , \\ \hat{A}_{\theta,\ell-1}(r) &= iC^{(\ell-1)}_{-}J_{\ell-2}(p_{n+1}r) - iC^{(\ell-1)}_{+}J_{\ell}(p_{n+1}r) \ , \end{aligned} \tag{61}$$

for $0 \leq r < R_0$. From Eqs. (47) and (48), we obtain

$$D^{+}_{\ell-1}(\omega,k)C^{(\ell-1)}_{+}J_{\ell}(\xi_{n+1}) = \frac{1}{2}\Lambda\sigma(\omega,k) \ , \tag{62}$$

and

$$D^{-}_{\ell-1}(\omega,k)C^{(\ell-1)}_{-}J_{\ell-2}(\xi_{n+1}) = \frac{1}{2}\Lambda\sigma(\omega,k) \ , \tag{63}$$

where the transverse dielectric functions $D^{+}_{\ell-1}(\omega,k)$ and $D^{-}_{\ell-1}(\omega,k)$ are defined by

$$D^{+}_{\ell-1}(\omega,k) = \frac{g_{\ell-1}(\zeta_{n+1})/\pi J_{\ell}(\xi_{n+1})}{g_{\ell-1}(\zeta_{n+1})N_{\ell}(\zeta_{n+1}) - J_{\ell}(\zeta_{n+1})} , \tag{64}$$

and

$$D^{-}_{\ell-1}(\omega,k) = - \frac{\zeta_{n+1}J_{\ell-1}(\zeta_{n+1})J'_{\ell-1}(\zeta_{n+1})}{J_{\ell}(\xi_{n+1})J_{\ell-2}(\xi_{n+1})} . \tag{65}$$

Substituting Eqs. (55) and (61) into Eq. (49), the source function $\sigma(\omega,k)$ can be expressed as

$$\sigma(\omega,k) = \chi_{n,n}\hat{\phi}_{\ell}(R_0) - 2\Lambda [\chi_{n,n-1}C^{(\ell+1)}_{-}J_{\ell}(\xi_{n-1}) + \chi_{n,n+1}C^{(\ell-1)}_{+}J_{\ell}(\xi_{n+1})] . \tag{66}$$

Equations (53), (56), (57), (60), and (63) constitute a set of linear algebraic equations relating $\hat{\phi}_{\ell}(R_0)$, $C^{(\ell+1)}_{\pm}$ and $C^{(\ell-1)}_{\pm}$. However, we note from Eq. (66) that the common source term $\sigma(\omega,k)$ is related only to the constants $\hat{\phi}_{\ell}(R_0)$, $C^{(\ell+1)}_{-}$, and $C^{(\ell-1)}_{+}$. In this regard, the equations containing $C^{(\ell+1)}_{+}$ and $C^{(\ell-1)}_{-}$ are completely decoupled from the remaining equations. Without loss of generality, Eqs. (56) and (63) are therefore omitted from the subsequent stability analysis. Making use of Eqs. (53), (57), and (62), we obtain the matrix equation relating $\hat{\phi}_{\ell}(R_0)$, $C^{(\ell-1)}_{+}J_{\ell}(\xi_{n+1})$, and $C^{(\ell+1)}_{-}J_{\ell}(\xi_{n-1})$, i.e.,

$$\begin{pmatrix} \Gamma_{\ell,n} + \frac{\pi}{2\gamma_b^2}\chi_{n,n} , & -\frac{\pi}{\gamma_b}\Lambda\chi_{n,n-1} , & -\frac{\pi}{\gamma_b}\Lambda\chi_{n,n+1} \\ -\frac{1}{2}\Lambda\chi_{n,n} , & D^{-}_{\ell+1} + \Lambda^2\chi_{n,n-1} , & \Lambda^2\chi_{n,n+1} \\ -\frac{1}{2}\Lambda\chi_{n,n} , & \Lambda^2\chi_{n,n-1} , & D^{+}_{\ell-1} + \Lambda^2\chi_{n,n+1} \end{pmatrix} \begin{pmatrix} \hat{\phi}_{\ell}(R_0) \\ C^{(\ell+1)}_{-}J_{\ell}(\xi_{n-1}) \\ C^{(\ell-1)}_{+}J_{\ell}(\xi_{n+1}) \end{pmatrix} = 0, \tag{67}$$

which is similar in general form to the matrix equation obtained by Uhm and Davidson[7] for the free electron laser instability associated with an annular electron beam propagating through an undulator multiple mirror magnetic field. Of course, the transverse dielectric functions $D^-_{\ell+1}$ and $D^+_{\ell-1}$ for a helical wiggler field are different from those for an undulator field.

The condition for a nontrivial solution to Eq. (67) is that the determinant of the matrix vanish. This gives the general dispersion relation

$$D^+_{\ell-1}D^-_{\ell+1}\left(\Gamma_{\ell,n} + \frac{\pi}{2\gamma_b^2}\chi_{n,n}\right) = -\Lambda^2(D^+_{\ell-1}\chi_{n,n-1} + D^-_{\ell+1}\chi_{n,n+1})\Gamma_{\ell,n} = 0 \ , \tag{68}$$

which can be used to determine the complex eigenfrequency ω in terms of $k + nk_0$, k_0, ν, Δ, and Λ.

IV. FREE ELECTRON LASER STABILITY PROPERTIES

We now investigate the free electron laser stability properties predicted by Eq. (68) for a relativistic annular electron beam propagating in a helical wiggler field. Consistent with Eqs. (5) and (9), the eigenfrequency ω can be approximated by $\omega \simeq (k+nk_0)V_b$. We therefore approximate $\zeta_{n+1} = \{\omega^2/c^2 - [k+(n+1)k_0]^2\}^{1/2}R_c$ by

$$\zeta_{n+1} = i\left[\frac{(k+nk_0)^2}{\gamma_b^2} + 2k_0(k+nk_0) + k_0^2\right]^{1/2} R_c \ . \tag{69}$$

After careful examination of Eq. (64) together with Eqs. (60) and (69), it is evident that the transverse dielectric function $D^+_{\ell-1}(\omega,k)$ is never equal to zero for $k + nk_0 \gtrless 0$. In this regard, for small wiggler amplitude ($\Lambda \ll 1$), we investigate free electron laser stability properties for ω and $(k + nk_0)$ near the simultaneous zeros of the ($\Lambda \to 0$) transverse dispersion relation $D^-_{\ell+1}(\omega,k) = 0$, and the ($\Lambda \to 0$) longitudinal dispersion relation $\Gamma_{\ell,n} + (\pi/2\gamma_b^2)\chi_{n,n} = 0$. For small but finite Λ, the general dispersion relation in Eq. (68) can then be approximated by the simplified form

$$D^-_{\ell+1}\left(\Gamma_{\ell,n} + \frac{\pi}{2\gamma_b^2}\chi_{n,n}\right) = -\Lambda^2\chi_{n,n-1}\Gamma_{\ell,n} \ . \tag{70}$$

Equation (70) is one of the principal results of this paper and can be used to investigate stability properties for a broad range of system parameters.

Making use of

$$p_n \simeq iq_n \equiv i(k + nk_0)/\gamma_b \ , \tag{71}$$

the longitudinal dielectric function $\Gamma_{\ell,n}$ can be expressed as

$$\Gamma_{\ell,n} = \frac{\pi}{2}\, h(q_nR_0) \quad \frac{\pi}{2}\, \frac{I_\ell(q_nR_c)/I_\ell(q_nR_0)}{I_\ell(q_nR_c)K_\ell(q_nR_0) - I_\ell(q_nR_0)K_\ell(q_nR_c)} \ , \tag{72}$$

for $k + nk_0 \geq 0$. In Eq. (72), $I_\ell(x)$ and $K_\ell(x)$ are modified Bessel functions of the first and second kind, respectively, of order ℓ, and $h(q_n R_0)$ is the effective longitudinal wave admittance. For short axial wavelengths with $(R_c - R_0)(k + nk_0) >> \gamma_b$, it is readily shown from Eq. (72) that the wave admittance h can be approximated by

$$h(q_n R_0) \simeq 2 \frac{k + nk_0}{\gamma_b} R_0 . \tag{73}$$

For free electron laser applications characterized by axial wavenumber $k + nk_0 \simeq (1 + \beta_b)\gamma_b^2 k_0$, Eq. (73) constitutes an excellent approximation.

For very small wiggler amplitude ($\Lambda \to 0$), or for very low beam density ($\nu \to 0$), it is evident from Eq. (70) that the linear dispersion relation for transverse perturbations is given by

$$\bar{D}_{\ell+1}(\omega,k) = 0, \tag{74}$$

and the linear dispersion relation for longitudinal perturbations is given by

$$\Gamma_{\ell,n}(\omega,k) + \frac{\pi}{2\gamma_b^2} \chi_{n,n} = 0 , \tag{75}$$

where $k + nk_0 \geq 0$ has been assumed. Making use of Eqs. (59) and (60), the dispersion relation in Eq. (74) can be expressed in the equivalent form

$$\frac{\omega^2}{c^2} - (k + nk_0 - k_0)^2 = \frac{\alpha_{\ell+1,s}^2}{R_c^2} , \tag{76}$$

for the transverse electric (TE) polarization, and

$$\frac{\omega^2}{c^2} - (k + nk_0 - k_0)^2 = \frac{\beta_{\ell+1,s}^2}{R_c^2} , \tag{77}$$

for the transverse magnetic (TM) polarization. In Eqs. (76) and (77), $\alpha_{\ell',s}$ is the s'th root of $J'_{\ell'}(\alpha_{\ell',s}) = 0$, and $\beta_{\ell',s}$ is the s'th root

of $J_{\ell'}(\beta_{\ell',s}) = 0$. Equations (76) and (77) are the familiar TE and TM mode dispersion relations for the vacuum waveguide modes.

For future reference, Taylor expanding the transverse dielectric function $D^{-}_{\ell+1}(\omega,k)$ in Eq. (59) about the vacuum waveguide results, it is straightforward to show that $D^{-}_{\ell+1}(\omega,k)$ can be approximated by

$$D^{-}_{\ell+1}(\omega,k) = \frac{R_c^2}{2\alpha^2_{\ell+1,s}}\left(\alpha^2_{\ell+1,s} - (\ell+1)^2\right)\left(\frac{J_{\ell+1}(\alpha_{\ell+1,s})}{J_\ell(\alpha_{\ell+1,s}R_0/R_c)}\right)^2 \times \left(\frac{\omega^2}{c^2} - (k + nk_0 - k_0)^2 - \frac{\alpha^2_{\ell+1,s}}{R_c^2}\right), \tag{78}$$

for the TE modes, and

$$D^{-}_{\ell+1}(\omega,k) = \frac{R_c^2}{2}\left(\frac{J'_{\ell+1}(\beta_{\ell+1,s})}{J_\ell(\beta_{\ell+1,s}R_0/R_c)}\right)^2 \times \left(\frac{\omega^2}{c^2} - (k + nk_0 - k_0)^2 - \frac{\beta^2_{\ell+1,s}}{R_c^2}\right), \tag{79}$$

for the TM modes.

In order to investigate the influence of axial momentum spread on the free electron laser instability, we assume an axial distribution function of the form

$$G(C_z) = \frac{\Delta}{\pi}\frac{1}{(C_z - \gamma_b mV_b)^2 + \Delta^2}, \tag{80}$$

where Δ is the characteristic spread in C_z about the mean value $\gamma_b mV_b$. We further assume that the spread Δ is small in comparison with $\gamma_b mV_b$, i.e., $\Delta \ll \gamma_b mV_b$. Substituting Eqs. (14), (34), and (80) into Eq. (39), we then obtain

$$\chi_{n,n'} = \frac{2\nu}{\gamma_b}\frac{\omega^2 - (k+nk_0)(k+n'k_0)c^2}{[\omega - (k+nk_0)V_b + i|k+nk_0|\Delta/\gamma_b^3 m]^2}, \tag{81}$$

within the context of Eqs. (6) and (9).

For small but finite wiggler amplitude and low beam density, we make use of Eqs. (72), (78), (79), and (81), to simplify the full dispersion relation in Eq. (70). This gives

$$\left\{\frac{\omega^2}{c^2} - (k + nk_0 - k_0)^2 - \frac{\alpha_{\ell+1,s}^2}{R_c^2}\right\}\left\{\left(\omega - (k+nk_0)V_b + i\frac{|k+nk_0|\Delta}{\gamma_b^3 m}\right)^2 - \frac{2\nu c^2}{\gamma_b^3 h}\left(2k_0(k+nk_0) - k_0^2 - \frac{\alpha_{\ell+1,s}^2}{R_c^2}\right)\right\} = 4\Lambda^2\frac{\nu c^2}{\gamma_b R_c^2}\left(k_0(k+nk_0-k_0) - \frac{\alpha_{\ell+1,s}^2}{R_c^2}\right) Q_{\ell s}^E(R_0/R_c) , \tag{82}$$

for the TE mode polarization, and

$$\left\{\frac{\omega^2}{c^2} - (k+nk_0-k_0)^2 - \frac{\beta_{\ell+1,s}^2}{R_c^2}\right\}\left\{\left(\omega - (k+nk_0)V_b + i\frac{|k+nk_0|\Delta}{\gamma_b^3 m}\right)^2 - \frac{2\nu c^2}{\gamma_b^3 h}\left(2k_0(k+nk_0) - k_0^2 - \frac{\beta_{\ell+1,s}^2}{R_c^2}\right)\right\} = 4\Lambda^2\frac{\nu c^2}{\gamma_b R_c^2}\left(k_0(k+nk_0-k_0) - \frac{\beta_{\ell+1,s}^2}{R_c^2}\right) Q_{\ell s}^M(R_0/R_c) , \tag{83}$$

for the TM mode polarization. In Eqs. (82) and (83), the TE and TM coupling coefficients, $Q_{\ell s}^E(R_0/R_c)$ and $Q_{\ell s}^M(R_0/R_c)$, are defined by

$$Q_{\ell s}^E(R_0/R_c) = \frac{\alpha_{\ell+1,s}^2}{\alpha_{\ell+1,s}^2 - (\ell+1)^2}\left(\frac{J_\ell(\alpha_{\ell+1,s}R_0/R_c)}{J_{\ell+1}(\alpha_{\ell+1,s})}\right)^2 \tag{84}$$

and

$$Q_{\ell s}^M(R_0/R_c) = \left(\frac{J_\ell(\beta_{\ell+1,s}R_0/R_c)}{J'_{\ell+1}(\beta_{\ell+1,s})}\right)^2 , \tag{85}$$

respectively. Equations (82) and (83) are the dispersion relations used in the remainder of this section, and can be used to investigate stability properties for a broad range of system parameters of experimental interest.

A careful examination of Eqs. (84) and (85) shows that the coupling between the transverse and longitudinal modes is maximum whenever $J'_\ell(\alpha_{\ell+1,s}R_0/R_c) = 0$ for the TE mode, and $J'_\ell(\beta_{\ell+1,s}R_0/R_c) = 0$ for the TM mode. Here, the prime (') denotes $dJ_\ell(x)/dx$. In this context, it is found that the maximum growth rate for perturbations with azimuthal harmonic number ℓ occurs for a value of R_0/R_c given by

$$R_0/R_c = \begin{cases} \alpha_{\ell,1}/\alpha_{\ell+1,s} , & \text{TE mode} , \\ \alpha_{\ell,1}/\beta_{\ell+1,s} , & \text{TM mode} , \end{cases} \tag{86}$$

where $\alpha_{\ell,1}$ is the first root of $J'_\ell(\alpha_{\ell,1}) = 0$. Equation (86) is valid only when $\alpha_{\ell,1} \leq \alpha_{\ell+1,s}$ for the TE mode, and $\alpha_{\ell,1} \leq \beta_{\ell+1,s}$ for the TM mode. For $\alpha_{\ell,1} > \alpha_{\ell+1,s}$ (TE), or $\alpha_{\ell,1} > \beta_{\ell+1,s}$ (TM), the maximum growth rate occurs for $R_0/R_c = 1$.

Shown in Fig. 1 are plots of (a) the ratio R_0/R_c that satisfies Eq. (86), and (b) the corresponding coupling coefficients $Q^E_{\ell s}$ and $Q^M_{\ell s}$ for several values of azimuthal and radial mode numbers, ℓ and s. Several points are noteworthy in Fig. 1. First, the maximum coupling occurs at $R_0/R_c = 1$ for the $(\ell,s) = (0,1)$ mode, where $\alpha_{0,1} = 3.83$, $\alpha_{1,1} = 1.84$ and $\beta_{1,1} = 3.83$. Second, except for azimuthally symmetric perturbations ($\ell = 0$), the value of R_0/R_c corresponding to maximum coupling increases with increasing mode numbers ℓ and s. Third, from Fig. 1(b), for a specified value of azimuthal harmonic number ℓ, the maximum coupling coefficients corresponding to the values of R_0/R_c in Eq. (86), increase rapidly with increasing radial mode number s. Finally, for specified values of (ℓ,s), we note from Fig. 1(b) that the maximum value of $Q^M_{\ell,s}$ is slightly larger than $Q^E_{\ell,s}$.

Defining the normalized Doppler-shifted eigenfrequency by

$$\Omega = [\omega - (k+nk_0)V_b]/k_0c \ , \tag{87}$$

we calculate the normalized growth rate $\Omega_i = \mathrm{Im}\Omega$ numerically from Eqs. (82) and (83) for a broad range of system parameters γ_b, ν/γ_b, Λ, $\Delta/\gamma_b mc$, R_0/R_c, ℓ, and s. Shown in Fig. 2 are plots of the normalized growth rate Ω_i versus $(k + nk_0)/k_0$ [Eqs. (82) and (83)] for $(\ell,s) = (1,3)$, $\gamma_b = 10$, $\nu/\gamma_b = 0.02$, $\Lambda^2 = 0.01$, $\Delta/\gamma_b mc = 0.002$, and $R_0/R_c = \alpha_{1,1}/\alpha_{2,3}$ for the TE mode, and $R_0/R_c = \alpha_{1,1}/\beta_{2,3}$ for the TM mode. It is evident from Fig. 2 that the TM mode is slightly more unstable than the TE mode, which is consistent with Fig. 1(b).

Shown in Fig. 3 are plots of the normalized TE mode growth rate Ω_i versus $(k + nk_0)/k_0$ obtained from Eq. (82) for $R_0/R_c = \alpha_{\ell,1}/\alpha_{\ell+1,s}$ [Eq. (86)]. The two plots correspond to (a) $\ell = 1$ and several values of s, and (b) $s = 3$ and several values of ℓ, and parameters otherwise identical to Fig. 2. As predicted in Fig. 1(b), it is evident from Fig. 3(a) that for a specified value of azimuthal mode number ℓ, the growth rate and range of k-space corresponding to instability increase rapidly with increasing radial mode number s. For R_0/R_c satisfying Eq. (86), we therefore conclude that perturbations with high radial mode numbers exhibit stronger instability than the fundamental mode (s=1). Moreover, the k-value corresponding to maximum growth is somewhat reduced as the radial mode number s is increased. For example, in Fig. 3(a), the maximum growth rate occurs at $k + nk_0 = 195\ k_0$ for $s = 1$, and at $k + nk_0 = 187\ k_0$ for $s = 5$. The maximum coupling coefficient in Fig. 1(b) decreases slowly with increasing azimuthal mode number ℓ, as does the instability growth rate [Fig. 3(b)]. The instability results for the TM mode are similar to those for the TE mode. However, the TM mode is somewhat more unstable than the TE mode.

V. CONCLUSIONS

In this paper, we have investigated the free electron laser stability properties for a relativistic annular electron beam propagating in combined transverse wiggler and uniform axial guide fields. The stability analysis has been carried out within the framework of the linearized Vlasov-Maxwell equations. The equilibrium properties and basic assumptions were summarized in Sec. II. The formal stability analysis was carried out in Sec. III for general azimuthal harmonic number ℓ, and a complete dispersion relation [Eqs. (68) or (70)] for the free electron laser instability was obtained, including the important influence of finite radial geometry. In Sec. IV, this dispersion relation was investigated for ω and $k + nk_0$ near the simultaneous zeros of the transverse and longitudinal dielectric functions. It was shown that the maximum coupling between the longitudinal and transverse modes occurs for values of R_0/R_c satisfying $R_0/R_c = \alpha_{\ell,1}/\alpha_{\ell+1,s}$ for the TE mode polarization, and $R_0/R_c = \alpha_{\ell,1}/\beta_{\ell+1,s}$ for the TM mode polarization. Moreover, the strength of the coupling increases considerably with increasing radial mode number s. It was also found that the TM mode is slightly more unstable than the TE mode.

ACKNOWLEDGMENTS

This research was supported in part by the Independent Research Fund at Naval Surface Weapons Center and in part by the Office of Naval Research.

APPENDIX A

ELECTROMAGNETIC POTENTIALS IN A CYLINDRICAL WAVEGUIDE

In this appendix, we investigate properties of the electromagnetic potentials in a cylindrical waveguide with radius R_c. Within the context of the Lorentz gauge condition,

$$\nabla \cdot \underset{\sim}{A}(\underset{\sim}{x},t) + \frac{1}{c}\frac{\partial}{\partial t}\phi(\underset{\sim}{x},t) = 0 \ , \tag{A.1}$$

the electromagnetic potentials, ϕ and $\underset{\sim}{A}$, are determined from the Maxwell equations

$$\left(\nabla^2 - \frac{1}{c^2}\frac{\partial^2}{\partial t^2}\right)\phi(\underset{\sim}{x},t) = -4\pi\rho(\underset{\sim}{x},t) \ ,$$

and

$$\left(\nabla^2 - \frac{1}{c^2}\frac{\partial^2}{\partial t^2}\right)\underset{\sim}{A}(\underset{\sim}{x},t) = -\frac{4\pi}{c}\underset{\sim}{J}(\underset{\sim}{x},t) \ , \tag{A.2}$$

where $\rho(\underset{\sim}{x},t)$ and $\underset{\sim}{J}(\underset{\sim}{x},t)$ are the charge and current densities, respectively, and c is the speed of light in vacuo. In the present analysis, we assume that all quantities vary with space and time according to

$$\psi(\underset{\sim}{x},t) = \hat{\psi}(r)\exp\{i(\ell\theta + kz - \omega t)\} \ , \tag{A.3}$$

where ℓ is the azimuthal harmonic number, k is the axial wavenumber, ω is the complex eigenfrequency, and $\hat{\psi}(r)$ is the amplitude. The components of the magnetic and electric fields can then be expressed as

$$\hat{B}_r(r) = i(\ell/r)\hat{A}_z(r) - ik\hat{A}_\theta(r) \ ,$$

$$\hat{B}_\theta(r) = ik\hat{A}_r(r) - (\partial/\partial r)\hat{A}_z(r) \ , \tag{A.4}$$

$$\hat{B}_z(r) = (1/r)(\partial/\partial r)(r\hat{A}_\theta) - (i/r)\ell\hat{A}_r(r) \ ,$$

and

$$\hat{E}_r(r) = -(\partial/\partial r)\hat{\phi}(r) + (i\omega/c)\hat{A}_r(r) ,$$

$$\hat{E}_\theta(r) = -(i\ell/r)\hat{\phi}(r) + (i\omega/c)\hat{A}_\theta(r) , \qquad (A.5)$$

$$\hat{E}_z(r) = -ik\hat{\phi}(r) + (i\omega/c)\hat{A}_z(r) .$$

Making use of Eq. (A.3), the Maxwell equations (A.2) can be expressed as

$$\left(\frac{1}{r}\frac{\partial}{\partial r} r \frac{\partial}{\partial r} - \frac{\ell^2}{r^2} + p^2\right)\hat{\phi}(r) = -4\pi\hat{\rho}(r) , \qquad (A.6)$$

$$\left(\frac{1}{r}\frac{\partial}{\partial r} r \frac{\partial}{\partial r} - \frac{\ell^2 + 1}{r^2} + p^2\right)\hat{A}_r(r) - \frac{2i\ell}{r^2}\hat{A}_\theta(r) = -\frac{4\pi}{c}\hat{J}_r(r) , \qquad (A.7)$$

$$\left(\frac{1}{r}\frac{\partial}{\partial r} r \frac{\partial}{\partial r} - \frac{\ell^2 + 1}{r^2} + p^2\right)\hat{A}_\theta(r) + \frac{2i\ell}{r^2}\hat{A}_r(r) = -\frac{4\pi}{c}\hat{J}_\theta(r) , \qquad (A.8)$$

and

$$\left(\frac{1}{r}\frac{\partial}{\partial r} r \frac{\partial}{\partial r} - \frac{\ell^2}{r^2} + p^2\right)\hat{A}_z(r) = -\frac{4\pi}{c}\hat{J}_z(r) , \qquad (A.9)$$

where p is defined by

$$p^2 = \omega^2/c^2 - k^2 . \qquad (A.10)$$

Introducing the new potential variables

$$\hat{A}_\pm(r) = \hat{A}_r(r) \pm i\hat{A}_\theta(r) , \qquad (A.11)$$

in Eqs. (A.7) and (A.8) gives

$$\left(\frac{1}{r}\frac{\partial}{\partial r} r \frac{\partial}{\partial r} - \frac{(\ell \pm 1)^2}{r^2} + p^2\right)\hat{A}_\pm(r) = -\frac{4\pi}{c}\hat{J}_\pm(r) , \qquad (A.12)$$

where the current densities $\hat{J}_\pm(r)$ are defined by $\hat{J}_\pm(r) = \hat{J}_r(r) \pm i\hat{J}_\theta(r)$.

In many charged particle beam applications, the perturbed charge density and axial current are related by

$$\hat{J}_z(r) = \eta c\hat{\rho}(r) \ , \tag{A.13}$$

where η is a constant. We therefore restrict the subsequent analysis to the case where Eq. (A.13) is satisfied. After a careful examination of Eq. (A.6), (A.9), and (A.13), we find that the axial component of vector potential is linearly proportional to $\hat{\phi}(r)$, i.e.,

$$\hat{A}_z(r) = \eta\hat{\phi}(r) \ . \tag{A.14}$$

Making use of Eqs. (A.1), (A.5), and (A.14), the appropriate boundary conditions at $r = R_c$ are given by

$$\hat{\phi}(R_c) = \hat{A}_z(R_c) = \hat{A}_\theta(R_c) = [(\partial/\partial r)(r\hat{A}_r)]_{r = R_c} = 0 \ , \tag{A.15}$$

provided

$$kc - \eta\omega \neq 0 \ . \tag{A.16}$$

Here, R_c is the radius of the conducting wall.

In a vacuum waveguide, where $\hat{\rho} = 0 = \hat{J}$, the solutions to Eqs. (A.6), (A.9), and (A.12) are given by

$$\hat{\phi}(r) = (1/\eta)\hat{A}_z(r) = \Phi J_\ell(pr) \ , \tag{A.17}$$

and

$$\hat{A}_\pm(r) = a_\pm J_{\ell\pm1}(pr) \ , \tag{A.18}$$

where Φ and $a_\pm$ are constants, and $J_\ell(x)$ is the Bessel function of the first kind of order ℓ. After some straightforward algebra that makes use of the definitions $\hat{A}_r = (\hat{A}_- + \hat{A}_+)/2$ and $\hat{A}_\theta = i(\hat{A}_- - \hat{A}_+)/2$, and the boundary condition $\hat{A}_\theta(R_c) = [(\partial/\partial r)(r\hat{A}_r)]_{R_c} = 0$ in Eq. (A.15), we obtain $a_+ = a_-$ in Eq. (A.18). Therefore, the radial and azimuthal components of the vector potential can be expressed as

$$\hat{A}_r(r) = a_+ \ell J_\ell(pr)/pr \ ,$$

$$\hat{A}_\theta(r) = ia_+ J'_\ell(pr) \ , \tag{A.19}$$

for $kc - \eta\omega \neq 0$. In Eq. (A.18), the prime (') denotes $(d/dx)J_\ell(x)$.

For an electromagnetic wave described by Eq. (A.19) with $a_+ \neq 0$, the boundary condition $\hat{A}_\theta(R_c) = 0$ implies

$$\frac{\omega^2}{c^2} - k^2 = \frac{\alpha_{\ell n}^2}{R_c^2} \ , \tag{A.20}$$

where $\alpha_{\ell n}$ is the nth root of $J'_\ell(\alpha_{\ell n}) = 0$. Equation (A.20) obviously satisfies Eq. (A.16). Moreover, from the boundary condition $\hat{\phi}(R_c) = 0$, we also note that the amplitude Φ satisfies $\Phi = 0$, which is consistent with the definition of the transverse electric (TE) mode polarization characterized by $\hat{E}_z(r) = 0$.

Similarly, for $\Phi \neq 0$, we find the transverse magnetic (TM) mode dispersion relation

$$\frac{\omega^2}{c^2} - k^2 = \frac{\beta_{\ell n}^2}{R_c^2} \ , \tag{A.21}$$

where $\beta_{\ell n}$ is the nth root of the Bessel function $J_\ell(\beta_{\ell n}) = 0$. Since $J'_\ell(\beta_{\ell n}) \neq 0$, the constant $a_+ = 0$ is required to satisfy the boundary condition $\hat{A}_\theta(R_c) = 0$, which is consistent with $\hat{B}_z(r) = 0$. From the Lorentz gauge condition in Eq. (A.1), we also find $\eta = \omega/kc$, and Eq. (A.16) can be expressed as $k^2c^2 - \omega^2 \neq 0$. To summarize, for a vacuum waveguide, the TM or TE modes are exclusively described by the potentials in Eq. (A.17) or Eq. (A.19), respectively.

As a second example, we calculate the electromagnetic dielectric function for the case where the radial and azimuthal current densities are given by

$$\hat{J}_r(r) = -i\hat{J}_\theta(r) = -\frac{c}{4\pi}\frac{\delta(r - R_0)}{R_0} K \ , \tag{A.22}$$

where R_0 and K are constants. In this case, Eqs. (A.7) and (A.8) can be expressed as

$$\left(\frac{1}{r}\frac{\partial}{\partial r} r \frac{\partial}{\partial r} - \frac{\ell^2+1}{r^2} + p^2\right)\hat{A}_r(r) - \frac{2i\ell}{r^2}\hat{A}_\theta(r) = \frac{\delta(r-R_0)}{R_0} K \ , \tag{A.23}$$

and

$$\left(\frac{1}{r}\frac{\partial}{\partial r} r \frac{\partial}{\partial r} - \frac{\ell^2+1}{r^2} + p^2\right)\hat{A}(r) + \frac{2i\ell}{r^2}\hat{A}_r(r) = \frac{\delta(r-R_0)}{R_0} iK \ . \tag{A.24}$$

Substituting Eq. (A.11) into Eqs. (A.23) and (A.24), it is found that the solutions to the coupled differential equations (A.23) and (A.24) are given by

$$\hat{A}_\pm(r) = 2\begin{cases} a_\pm J_{\ell\pm1}(pr) + b_\pm N_{\ell\pm1}(pr) \ , & R_0 < r \le R_c \ , \\ C_\pm J_{\ell\pm1}(pr) \ , & 0 \le r < R_0 \ , \end{cases} \tag{A.25}$$

where the constants $a_\pm$, $b_\pm$ and $C_\pm$ are determined by the boundary conditions that the potentials $\hat{A}_\theta(r)$ and $\hat{A}_r(r)$ are continuous at $r = R_0$, and that $\hat{A}_\theta(r)$ and $(\partial/\partial r)(r\hat{A}_r)$ vanish at $r = R_c$. According to Eq. (A.11), Eq. (A.25) can also be expressed as

$$A_r(r) = \begin{cases} a_- J_{\ell-1}(pr) + b_- N_{\ell-1}(pr) + a_+ J_{\ell+1}(pr) + b_+ N_{\ell+1}(pr) \ , \\ \qquad R_0 < r \le R_c \ , \\ C_- J_{\ell-1}(pr) + C_+ J_{\ell+1}(pr) \ , \quad 0 \le r < R_0 \ , \end{cases} \tag{A.26}$$

and

$$A_\theta(r) = i\begin{cases} a_- J_{\ell-1}(pr) + b_- N_{\ell-1}(pr) - a_+ J_{\ell+1}(pr) - b_+ N_{\ell+1}(pr) \ , \\ \qquad R_0 < r \le R_c \ , \\ C_- J_{\ell-1}(pr) - C_+ J_{\ell+1}(pr) \ , \quad 0 \le r < R_0 \ . \end{cases} \tag{A.27}$$

Multiplying Eqs. (A.23) and (A.24) by r and integrating from $R_0(1-\varepsilon)$ to $R_0(1+\varepsilon)$, with $\varepsilon \to 0_+$, we obtain after some straightforward algebra,

$$D_\ell^+(\omega,k) C_+ J_{\ell+1}(\xi) = \frac{1}{2} K \ , \tag{A.28}$$

and

$$D_\ell^-(\omega,k)C_- J_{\ell-1}(\xi) = \frac{1}{2} K \ , \tag{A.29}$$

where the dielectric functions $D_\ell^+(\omega,k)$ and $D_\ell^-(\omega,k)$ are defined by

$$D_\ell^+(\omega,k) = - \frac{\zeta J_\ell(\zeta) J'_\ell(\zeta)}{J_{\ell-1}(\xi) J_{\ell+1}(\xi)} \ , \tag{A.30}$$

and

$$D_\ell^-(\omega,k) = \frac{2J_\ell(\zeta)J'_\ell(\zeta)/\pi J_{\ell-1}(\xi)}{2J_\ell(\zeta)J'_\ell(\zeta)N_{\ell-1}(\xi) - [J_\ell(\zeta)N'_\ell(\zeta) + J'_\ell(\zeta)N_\ell(\zeta)]J_{\ell-1}(\xi)} \ . \tag{A.31}$$

Here, $\xi = pR_0$ and $\zeta = pR_c$.

In a similar manner, we also obtain Eqs. (A.28) and (A.29) in circumstances where the radial and azimuthal current densities are related by

$$\hat{J}_r(r) = i\hat{J}_\theta(r) = - \frac{c}{4\pi} \frac{\delta(r-R_0)}{R_0} K \ . \tag{A.32}$$

In this case, however, the dielectric functions are defined by

$$D_\ell^+(\omega,k) = \frac{2J_\ell(\zeta)J'_\ell(\zeta)/\pi J_{\ell+1}(\xi)}{2J_\ell(\zeta)J'_\ell(\zeta)N_{\ell+1}(\xi) - [J_\ell(\zeta)N'_\ell(\zeta) + J'_\ell(\zeta)N_\ell(\zeta)]J_{\ell+1}(\xi)} \ , \tag{A.33}$$

and

$$D_\ell^-(\omega,k) = - \frac{\zeta J_\ell(\zeta) J'_\ell(\zeta)}{J_{\ell+1}(\xi) J_{\ell-1}(\xi)} \ . \tag{A.34}$$

REFERENCES

1. T. C. Marshall, S. Talmadge, and P. Efthimion, Appl. Phys. Lett. 31, 320 (1977).
2. D. A. G. Deacon, L. R. Elias, J. M. M. Madey, G. J. Ramian, H. A. Schwettman, and T. I. Smith, Phys. Rev. Lett. 38, 897 (1977).
3. R. C. Davidson and H. S. Uhm, Phys. Fluids 23, in press (1980).
4. A. T. Lin and J. M. Dawson, Phys. Fluids 23, 1224 (1980).
5. P. Sprangle, C. M. Tang, and W. M. Manheimer, Phys. Rev. A21, 302 (1980).
6. I. B. Bernstein and J. L. Hirshfield, Phys. Rev. A20, 1661 (1979).
7. H. S. Uhm and R. C. Davidson, "Theory of Free Electron Laser Instability in a Relativistic Annular Electron Beam", submitted for publication (1980).
8. R. C. Davidson and H. S. Uhm, "Helically Distorted Relativistic Electron Beam Equilibria for Free Electron Laser Applications", submitted for publication (1980).

FIGURE CAPTIONS

Fig. 1 Plots of (a) the ratio R_0/R_c satisfying Eq. (86), and (b) the corresponding coupling coefficients $Q^E_{\ell s}$ and $Q^M_{\ell s}$ for several values of azimuthal and radial mode numbers, ℓ and s.

Fig. 2 Plots of normalized growth rate Ω_i versus $(k + nk_0)/k_0$ [Eqs. (82) and (83)] for $(\ell,s) = (1,3)$, $\gamma_b = 10$, $\nu/\gamma_b = 0.02$, $\Lambda^2 = 0.01$, $\Delta/\gamma_b mc = 0.002$, and R_0/R_c satisfying Eq. (86).

Fig. 3 Plots of normalized TE mode growth rate Ω_i versus $(k + nk_0)/k_0$ [Eq. (82)] for $R_0/R_c = \alpha_{\ell,1}/\alpha_{\ell+1,s}$, (a) $\ell = 1$ and several values of s, (b) $s = 3$ and several values of ℓ, and parameters otherwise identical to Fig. 2.

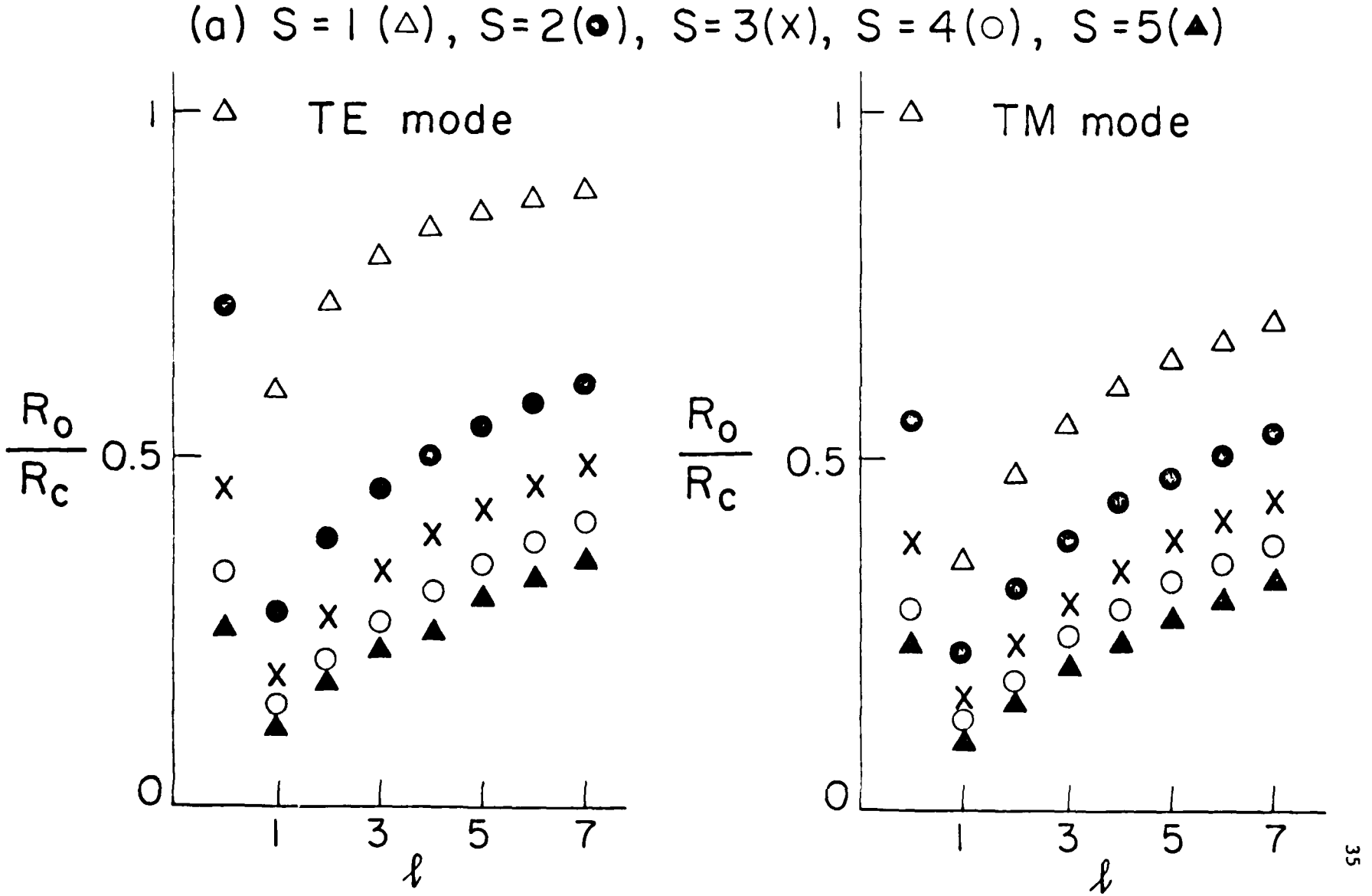

Fig. 1(a)

(b) S = 1 (△), S = 2 (●), S = 3 (x), S = 4 (○), S = 5 (▲)

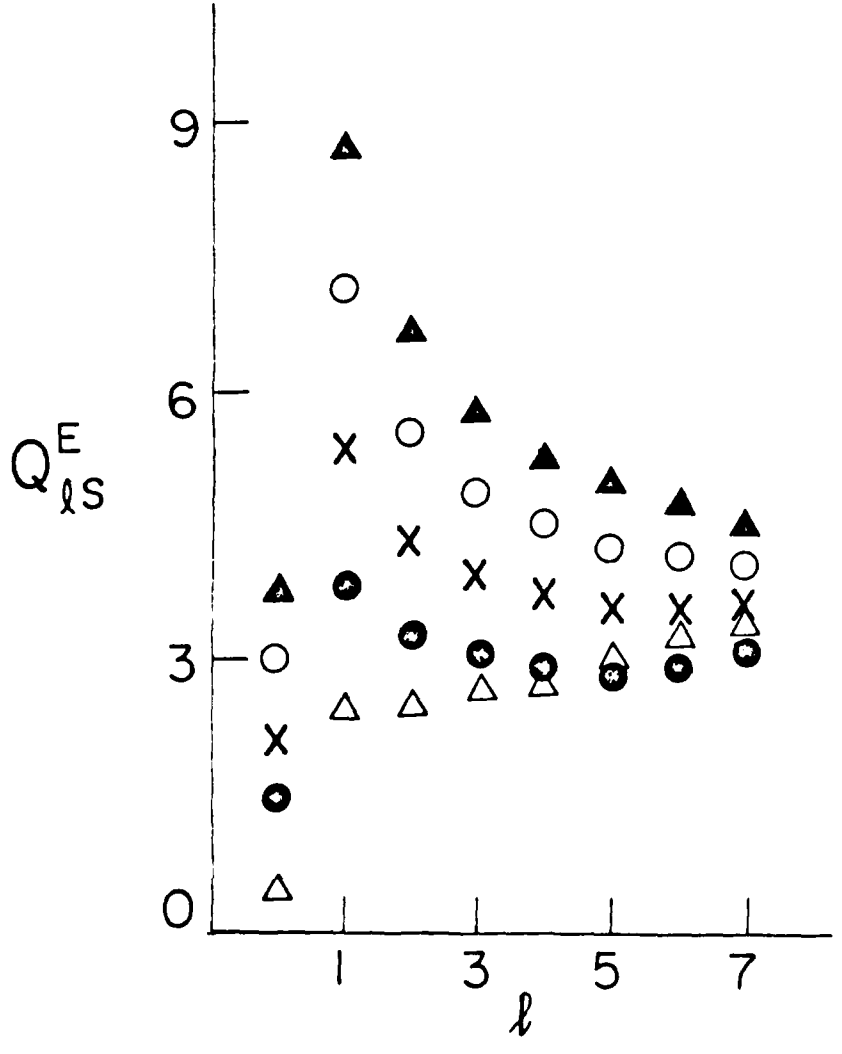

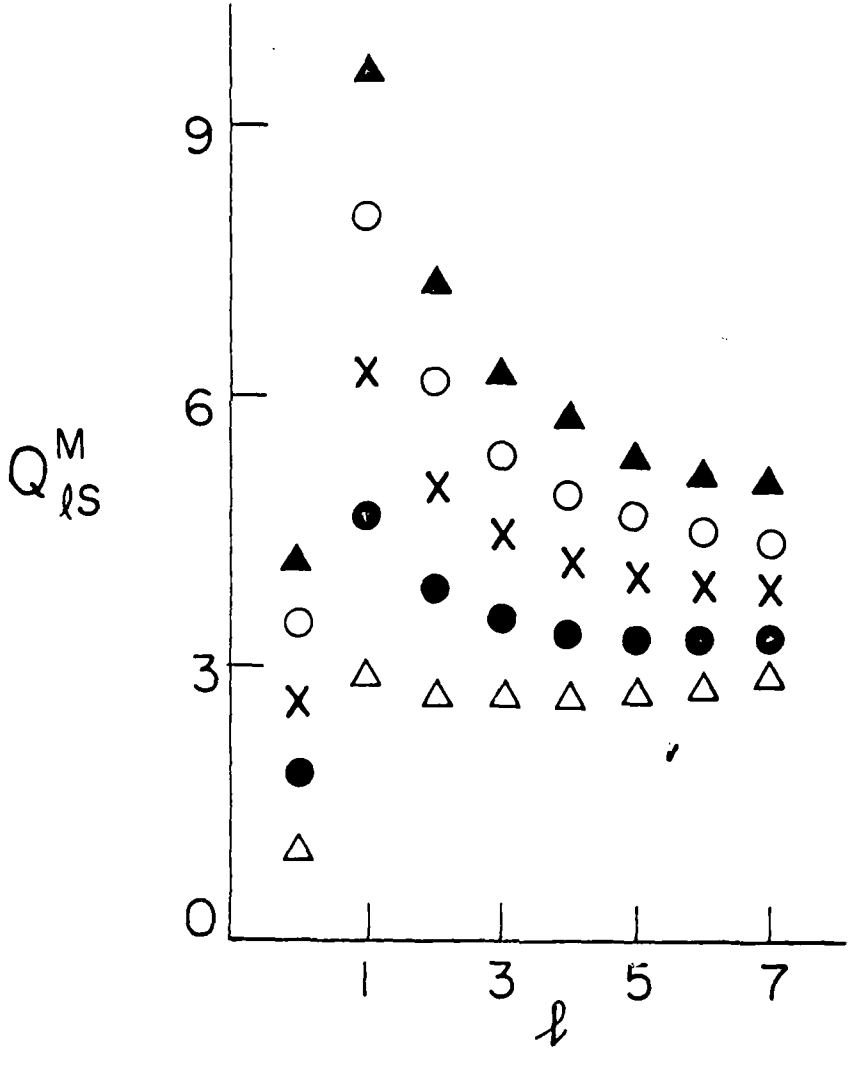

Fig. 1(b)

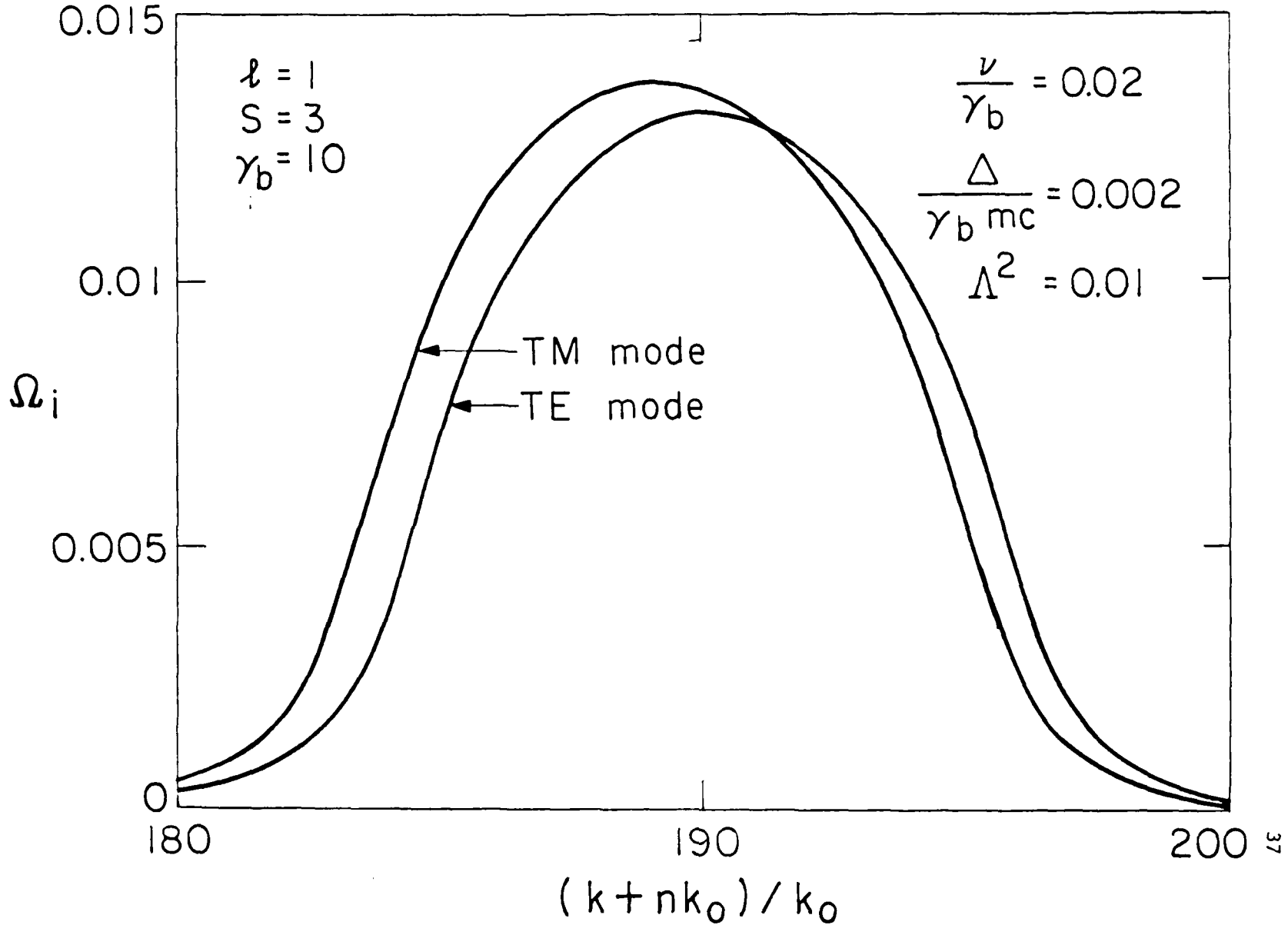
0.015
0.01
0.005
0
Ω_i
$\ell = 1$
$S = 3$
$\gamma_b = 10$
$\frac{\nu}{\gamma_b} = 0.02$
$\frac{\Delta}{\gamma_b mc} = 0.002$
$\Lambda^2 = 0.01$
TM mode
TE mode
180
190
200
$(k + nk_o)/k_o$

Fig. 2

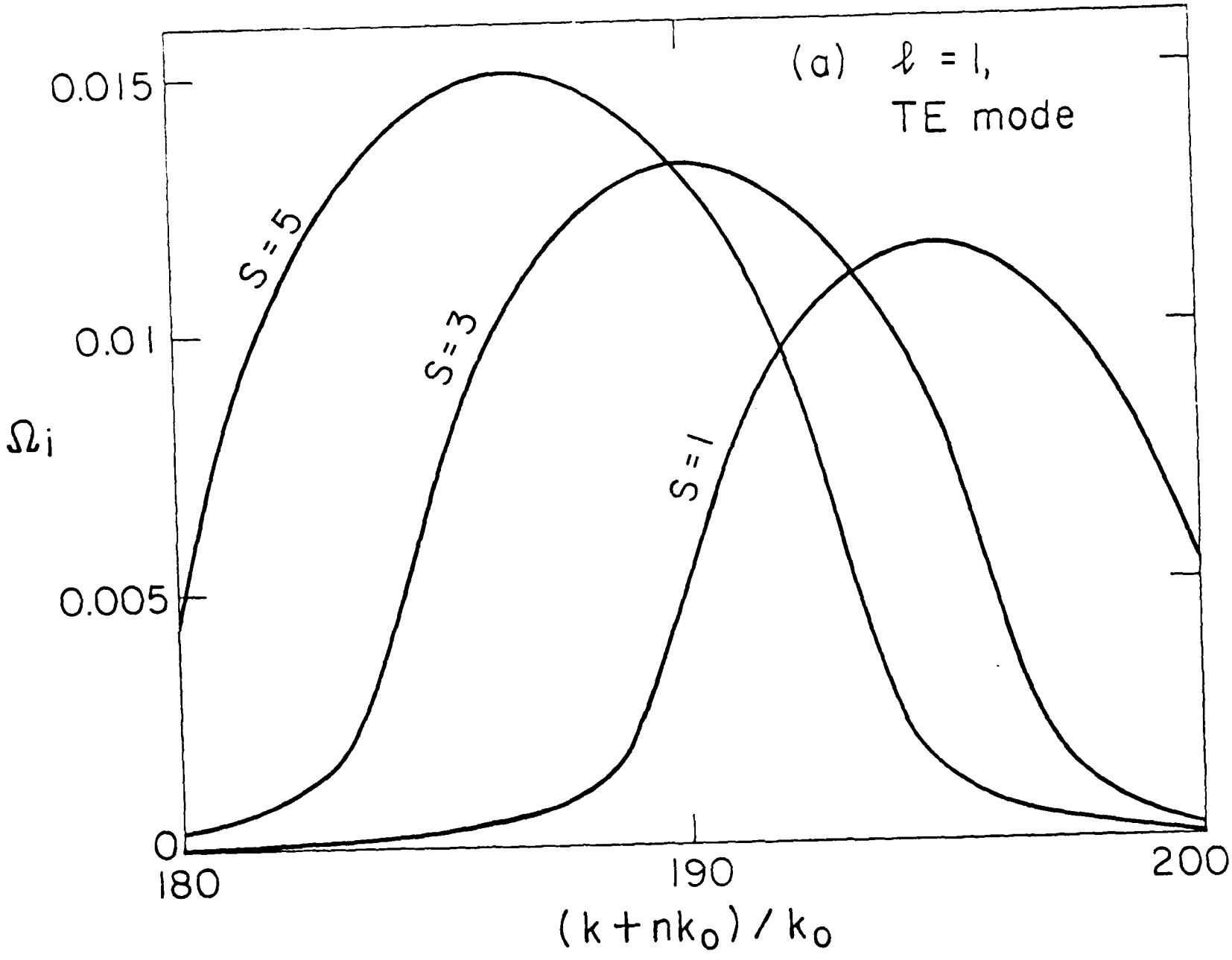

Fig. 3(a)

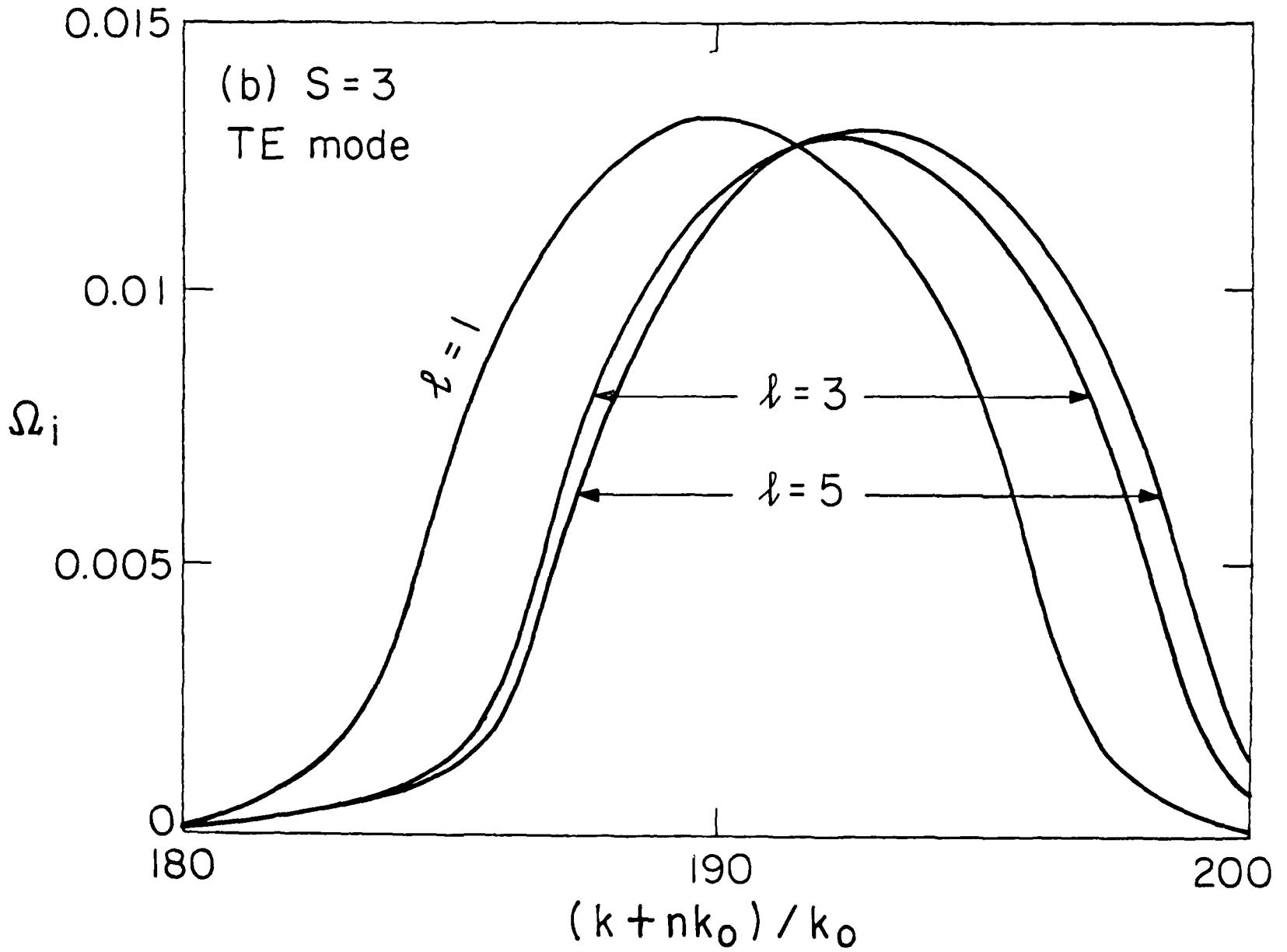
0.015
(b) S = 3
TE mode
0.01
Ω_i
$\ell = 1$
$\ell = 3$
$\ell = 5$
0.005
0
180
190
200
$(k + nk_o) / k_o$

Fig. 3(b)

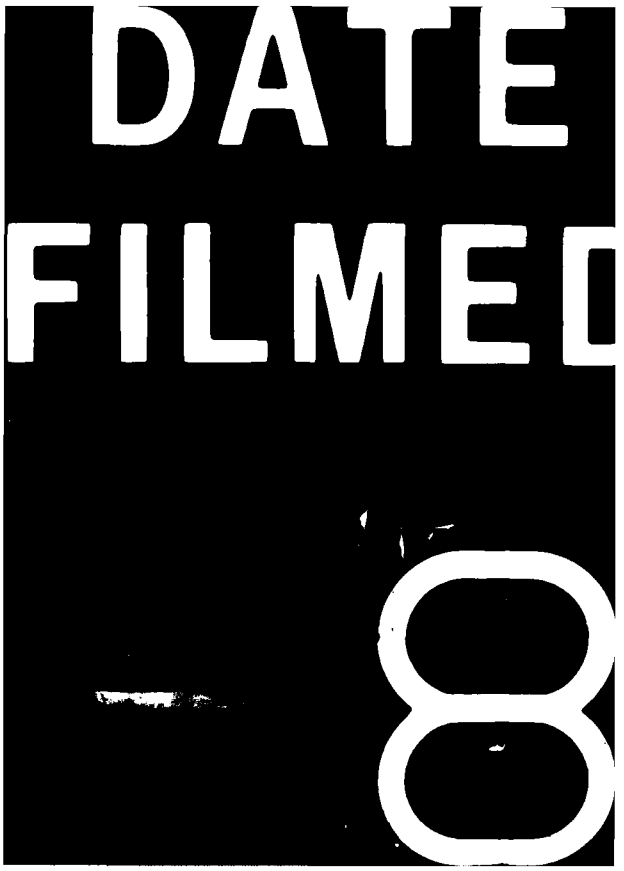
DATE
FILMED
8